JNCC Report No. 676

Copernicus User Uptake (CUU): Applying Earth Observation (EO) to horizon scanning for Emerging Infectious Diseases (EIDs)

Day, J.[1], Ashfield, S.[2], Brown, D.[2], Gale, P.[2], Heeley, L.[1], Snary, E.[2], Taylor, R.[2], Way, L.[1] & Jones, G.[1]

May 2021

ISSN 0963 8091

For further information please contact:
Joint Nature Conservation Committee
Monkstone House
City Road
Peterborough PE1 1JY
https://jncc.gov.uk/

This report should be cited as:
Day, J., Ashfield, S., Brown, D., Gale, P., Heeley, L., Snary, E., Taylor, R., Way, L. & Jones, G. 2021. Copernicus User Uptake (CUU): Applying Earth Observation (EO) to horizon scanning for Emerging Infectious Diseases (EIDs). *JNCC Report No. 676*, JNCC, Peterborough, ISNN 0963-8091.

Acknowledgements
JNCC would like to thank our partners at Animal Plant Health Agency for their valuable input in to shaping and reviewing this report. With special thanks to Andy Hardy at Aberystwyth University for providing useful insight and suggestions in reviewing this report.

This project was funded by the Caroline Herschel framework Partnership Agreement on Copernicus User Uptake on Copernicus User Uptake and the Versatile emerging infectious disease observatory: Forecasting, nowcasting and tracking in a changing world. VEO has received funding from the European Union's Horizon 2020 research and innovation programme under grant agreement No. 874735

EQA:
This report is compliant with JNCC's Evidence Quality Assurance Policy
https://jncc.gov.uk/about-jncc/corporate-information/evidence-quality-assurance/

Affiliation:
[1]Joint Nature Conservation Committee, Peterborough, UK
[2] Department of Epidemiological Sciences, Animal & Plant Health Agency, UK

Contents

1 Introduction

This report details the outcomes of a desk study to explore the possibility for using Earth Observation (EO) in horizon scanning for Emerging Infectious Disease (EIDs). EO refers to methods for remotely sensing the environment. This can be done through using different types of sensors, including those on satellites in space or those aboard aircraft. EIDs refer to infectious diseases that are newly identified or that are likely to increase their geographical range. For the purposes of this desk study, infectious diseases are only considered if they affect livestock, have wildlife reservoirs or impact human health.

The report starts with a case study showcasing how EO has and could be used with West Nile Virus. The report then reviews six broad drivers for EIDs, which were identified by the Animal and Plant Health Agency (AHPA) as part of the Versatile Emerging infectious disease Observatory (VEO) project. The broad drivers are human, wildlife, livestock, composition of landscape and land use, climate/weather, and zoological/virological (including vector species). Each of the broad drivers are broken down into further drivers (Table 1). Under each driver, a short description and illustrative examples are given from the literature of how EO has and could be used as a data source. Where possible, as data products are listed in tables, they are colour coded according to a key which broadly indicates how accessible those products are likely to be (Table 2) for practitioners evaluation risk around EIDs, including staff at APHA.

Table 1. Drivers of EIDs explored in this report. There are six main drivers and each driver is split up into further sub drivers.

Main driver	Sub driver
Human	• Population change • Globalisation – movement of people and goods
Wildlife	• Wildlife population change • Wildlife management practices • Wildlife moved for hunting • Exposure to wildlife at wet markets • Exposure to wildlife – subsistence hunting • Exposure to wildlife – ecotourism • Exposure to wildlife viruses directly via livestock
Livestock	• Livestock population change • Livestock management practices • Movement of wildlife • Exposure to livestock at wet markets • Exposure to livestock ticks • Butchering of livestock
Composition of landscape and land use	• Fragmentation of landscape and land use • Land use and farm management
Climate / Weather	• Climate change over time • Climate change range expansion • Weather patterns (seasonal)
Zoological / Virological	• Monitoring of Invasive species • Change in abundance / range of reservoirs, and vectors • Adaptation to new environment (vectors / virus)

Table 2. The colour coding system used throughout this report to indicate how accessible EO data are to all.

Colour	Accessibility
Green	Data product available for free
Orange	Data product available for a cost
Red	Data product not available
White	Not assessed due to time constraints

Data derived from EO is of great interest for work on EIDs as they can offer continuous spatial and temporal coverage. This has the added benefits for EIDs that there will often be historical data which can be used to explore the relationship EIDs have with the environment and that there will usually be global datasets available to study an EID that is not yet in the UK or Europe.

2 Case study: West Nile Virus

West Nile Virus (WNV) is spread by mosquitos and can cause neurological diseases and death in humans. Although commonly found in Africa, the Middle East, North America and West Asia, there have been several recent outbreaks of WNV in Europe (see Figure 1 for infections in Europe during 2020). Birds act as the primary host for WNV and migrating birds have been linked to the geographic spread of the virus. Humans and horses (and other mammals) act as dead-end hosts for WNV (Figure 2 illustrates the transmission route for WNV).

2.1 Risk/probability of establishment

Current approaches in predicting the risk/probability of WNV establishing in Europe and the UK include using vector trait data (e.g. bite rate, longevity) paired with environmental variables such as monthly temperature. EO can be used to help map the risk or probability of a disease establishing in a new area. Examples of EO data that have been used in this respect are listed below. Often a number of these are used together to assess the risk of establishment:

- **Land surface temperature (LST)** has been linked to the incubation period of WNV (Liu & Weng, 2012) and has been correlated with infection (160 days prior to infection, Candeloro *et al.* 2020)
- **Surface Soil Moisture (SSM)** has been correlated with infection (160 days prior to infection, Candeloro *et al.* 2020)
- **Normalised Difference Vegetation Index (NDVI)** has been correlated with infection (160 days prior to infection, Candeloro *et al.* 2020)
- **Land cover** has been an important factor for WNV risk in horses, with high risk areas having low tree, water and wetland cover (Epp *et al.* 2010).

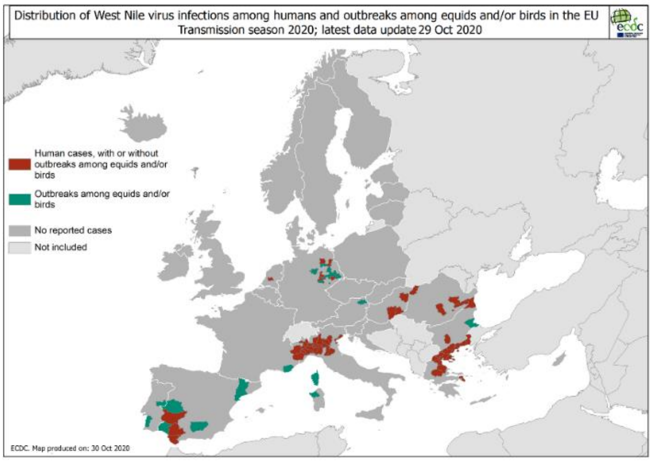

Figure 1. European infection cases during 2020 (up until 29 October 2020) in humans (red) and birds and horses/equids (green). Map produced by European Centre for Disease Prevention and Control.

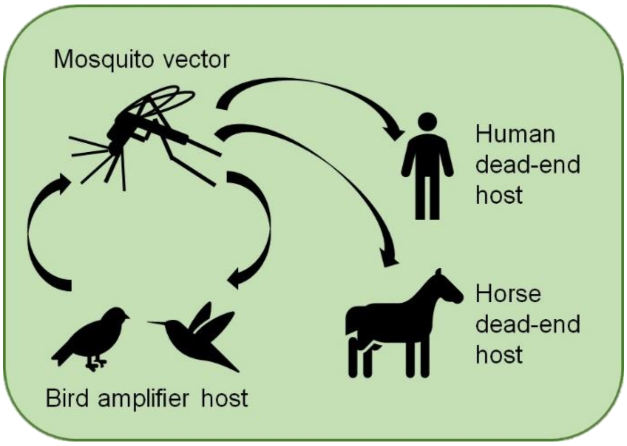

Figure 2. Transmission route of WNV.

3 Human drivers

The first main driver explored here are human drivers, which were identified as important for informing EIDs, specifically around **human population change** and **globalisation** (the movement of people and goods, Table 1). There are several proxies and models using EO inputs that can be used to monitor human population change which are listed in Table 3. These proxies and data products that are derived from EO are particularly useful as traditional methods to monitor human population change, such as using census counts, are resource intense, can be incomplete and can quickly become out of date.

3.1 Human population change

Earth Observation can be used as the main source of data for human population estimates or it can be combined with other data. People have used EO for at least half a century to produce figures on human populations, for instance using aerial photography (see Anderson & Anderson 1973). A more commonly used proxy for human population is night-time lighting, derived from satellite images (Sutton 2001). Night-time lighting can regularly be captured through satellites at a global scale. These images can be used to track changes in light emissions which has been linked to changes in human population. An example is shown in Figure 4 with a visible increase in light levels in China from 1992 to 2008.

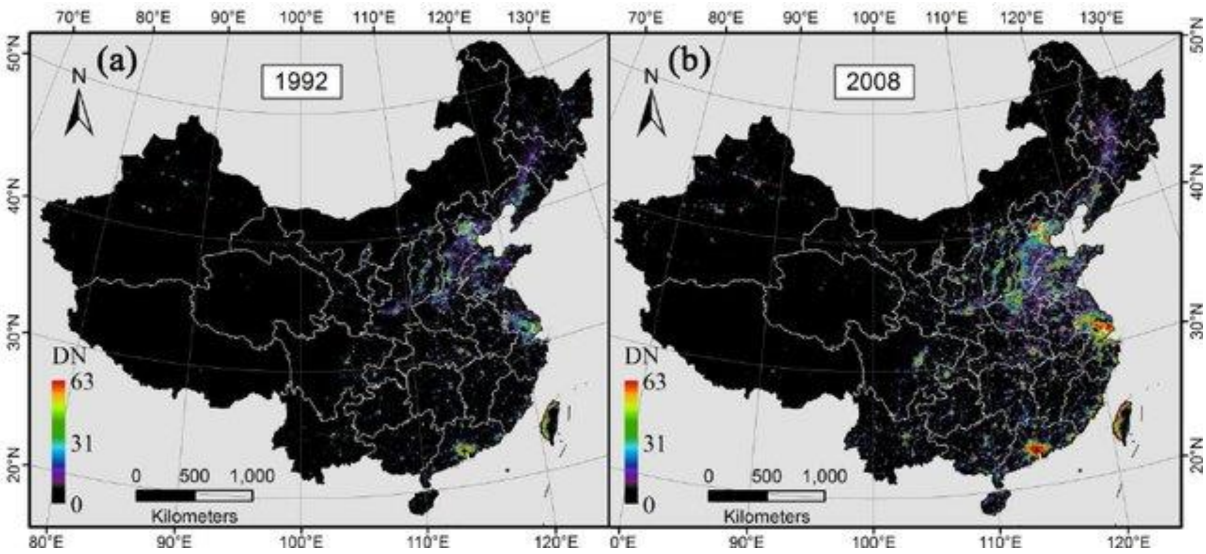

Figure 3. Night time lighting in China 1992 (left) and 2008 (right) taken from Liang *et al.* 2014. Light levels are derived from The Defense Meteorological Program (DMSP) Operational Line-Scan System (OLS) where a DN value of 0 indicates no light and 63 maximum light levels.

Another way to use EO for data on human population change is to combine it with other data sources (e.g. Figure 5), which is particularly useful for improving census population estimates (see *Azar et al.* 2010; Linard *et al*. 2011 for applied examples). This produces products which can be used to explore the relationship between risk of infectious disease and human population (Balk *et al.* 2006).

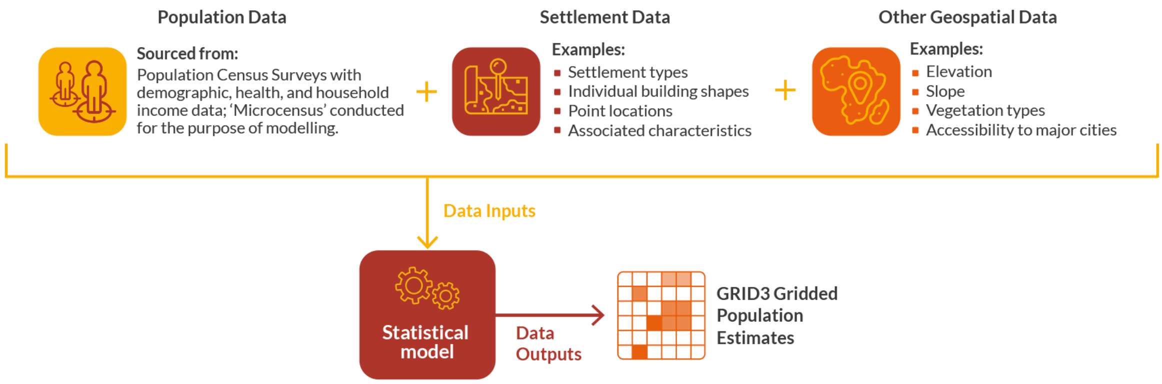

Figure 4. An example of a modelled approach to combine census data with data derived from Earth Observations (e.g. settled and geospatial data). Taken from the Geo-Referenced Infrastructure and Demographic Data for Development (GRID[3]).

3.2 Globalisation

This section is split in to two. First, EO that can be used to capture human consumption and secondly, EO that can be used to detect the movement of goods. There are a number of proxies that can be used to represent human consumption (detailed in Table 3). For illustrative purposes, Human footprint maps using the Last of the Wild Project datasets are show in Figure 6. These maps are produced by combining several EO datasets: the built environment (DMSP-OLS), human population density (GPW), Night-time lights (DMSP-OLS), crop and pasture lands (UMD Land Cover Classification and GlobCover), roads and railways (gROADS), navigable waters (navigable waters within 80km of a lit area identified using DMSP-OLS). The acronyms of these satellites and data products are expanded in the caption of Table 3. These maps are currently only available for two years (1993 and 2009) but illustrate what could be produced using EO.

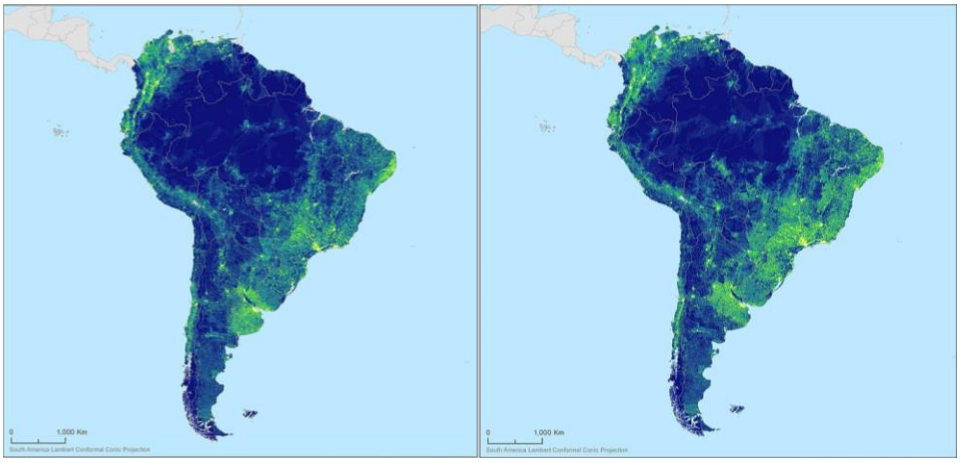

Figure 5. Last of the Wild Project, Version 3 (LWP-3). The map shows human pressure in South America for 1993 (left) and 2009 (right) with dark blue representing low human pressure shading up to yellow for high human pressure (Venter *et al.* 2018a; 2018b).

Table 3. Human drivers for EIDs. Proxies that can be derived from Earth Observation data, satellites and sensors that provide appropriate data, data products available (if applicable) and applied examples. Acronyms given in the table below for satellites and sensors are expanded here: Advanced Very High-Resolution Radiometer (AVHRR); International Satellite Land Surface Climatology Project *initiative II* (ISLSCP II). Acronyms given in the table below for organisations are expanded here: Level-1 and Atmospheric Archive & Distribution System (LAADS); National Oceanic and Atmospheric Administration (NOAA); Socioeconomic Data and Applications Center (SEDAC). Colours indicate how accessible the EO data are: green (data product available for free), orange (data product available for a cost), red (data product not available), white (not assessed).

Driver	Proxy	Data product	Satellite (sensor) / EO	Spatial coverage	Temporal coverage	Examples
Population change	Night-time light	Night-time Lights Time Series from NOAA	DMSP (OLS)	Global 3km	1993-2014	Li & Zhou (2017) reviewed the used of DMSP-OLS data to map urbanisation. Wang *et al*. (2000a) used GMSP-OLS data combined with land class maps to classify and track changes in levels of urbanisation in China.
		VNP46A1 and VNP46A2 from NASA LAADS	Suomi NPP (VIIRS DNB)	Global 15 arc seconds	2012-present Daily	
	Human population models	LandScan	Incorporates landcover data from a range of sources e.g. USGS, NASA, and NOAA	Global ~1km	1998 and 2000-2018 Annual	Hay *et al*. (2005b) compared human population from GPW and LandScan to census data for risk of malaria transmission in Kenya and in Hay *et al*. (2005a) identified that rates of malaria are lower in urban areas.
		Gridded Population of the World (GPW) v4 from SEDAC		Global 2.5 arc-minute	Estimates for these years: 1990, 1995, 2000	
		Global Rural-Urban Mapping Project (GRUMP) v1 from SEDAC	Incorporates date from DMSP (OLS)	Global 30 arc-second	Estimates for these years: 1990, 1995, 2000	

Driver	Proxy	Data product	Satellite (sensor) / EO	Spatial coverage	Temporal coverage	Examples
		Geo-Referenced Infrastructure and Demographic Data for Development (GRID3)		Some African countries	Dependant on data product	
Globalisation – movement of people and goods	Human consumption	Human Appropriation of Net Primary Productivity (HANPP) from SEDAC	Model incorporates data from a range of EO sensors including AVHHR and ISLSCP II	Global 0.25 decimal degrees	1995	Imhoff & Bounoua (2006) describe the method for produce the HANPP global dataset.
		Human footprint map from SEDAC		Global ~1 km	1993, 2009	
		Night-time Lights Time Series from NOAA	*See above under night-time light.*			Wang *et al.* (2000a) used night-time light levels as a measure of urbanisation to evaluate Mainland China consumption in response to the Sustainable Development Goal 11.3.1.
		VNP46A1 and VNP46A2 from NASA LAADS				
	Movement of goods - ship detection and port activity	Search for Unidentified Maritime Objects (SUMO) algorithm	Can be used with a range of Synthetic Aperture Radar (SAR) satellites including Sentinel-1	Global		The main methods for tracking ships are Automatic Identification Systems (AIS) (Lee *et al*. 2019). These systems do not rely on EO, however are complimented by EO. Where vessel do not use AIS or are carrying out illegal activity, EO can provide

Driver	Proxy	Data product	Satellite (sensor) / EO	Spatial coverage	Temporal coverage	Examples
						helpful additional information using methods such as SUMO. Greidanus *et al.* (2017) describes the SUMO algorithm. Grover *et al.* (2018) used the SUMO algorithm to test whether Sentinel-1 data could be used to track ships. Snapir *et al.* (2019) used the SUMO algorithm and Random Forest models to distinguish fishing and non-fishing vessels using Sentinel-1 data.
		Night-time Lights Time Series from NOAA	*See above under night-time light.*			Zhang et al. (2017) used night-time light data to identify ships fishing Japanese common squid in coastal waters of Japan. Li *et al.* (2017) compared DMSP-OLS data and port economic comprehensive scores for major cities in China.
		VNP46A1 and VNP46A2 from NASA LAADS				
	Movement of goods - Roads	gROADS	Incorporates imagery and data products from a range of satellites.	Global Map scale of ~1:1m	One dataset for 1980-2010	

4 Wildlife drivers

Data on wildlife drivers is the next main driver explored here which was identified as important for informing EIDs (Table 1), specifically around **wildlife population change**, **wildlife management practices**, **wildlife moved for hunting**, **exposure to wildlife at wet markets**, **exposure to wildlife through subsistence hunting**, **exposure to wildlife through ecotourism** and **exposure to wildlife viruses directly via livestock**.

4.1 Wildlife population change

Note that this section of the report deals broadly with the topic wildlife animals and does not go into detail about vectors and reservoirs of disease as this is covered in the section under the final section of zoological/virological drivers. There is some overlap between these two sections.

There are both direct and indirect methods for detecting wildlife population change from EO. Direct measures are often produced using imagery from Unmanned Aerial Vehicle (UAVs, see Table 4), however can also be produced using manned aerial surveys and satellites (see Wang *et al.* 2019 for a review and comparison of these methods). Manned aerial surveys and UAVs can be fitted with different types of camera, for example spectral or thermal. UAVs tend to be more popular than manned surveys as the technology is cheaper and more cost effective to run and repeat surveys. Aerial surveys tend to only be appropriate for some animals, for example large ones or ones that stand out from their backgrounds. Christie *et al.* (2016) have a useful review of studies estimating population size and other metrics from UAVs, with animals covered including sperm whales, walrus, sea turtles, penguins, sandhill crane, flamingos, beaver, elephant and orangutans. Figure 7 demonstrates the process of going from a UAV, to images and then to population estimates for wild herbivores. It should be noted that monitoring and predicting disease expansion often requires large scale data and so the direct measurements of wildlife population change described here (which are typically appropriate for small scale monitoring) may not be appropriate. In this context, alternative indirect measures of wildlife population change at a larger scale are likely to be more important.

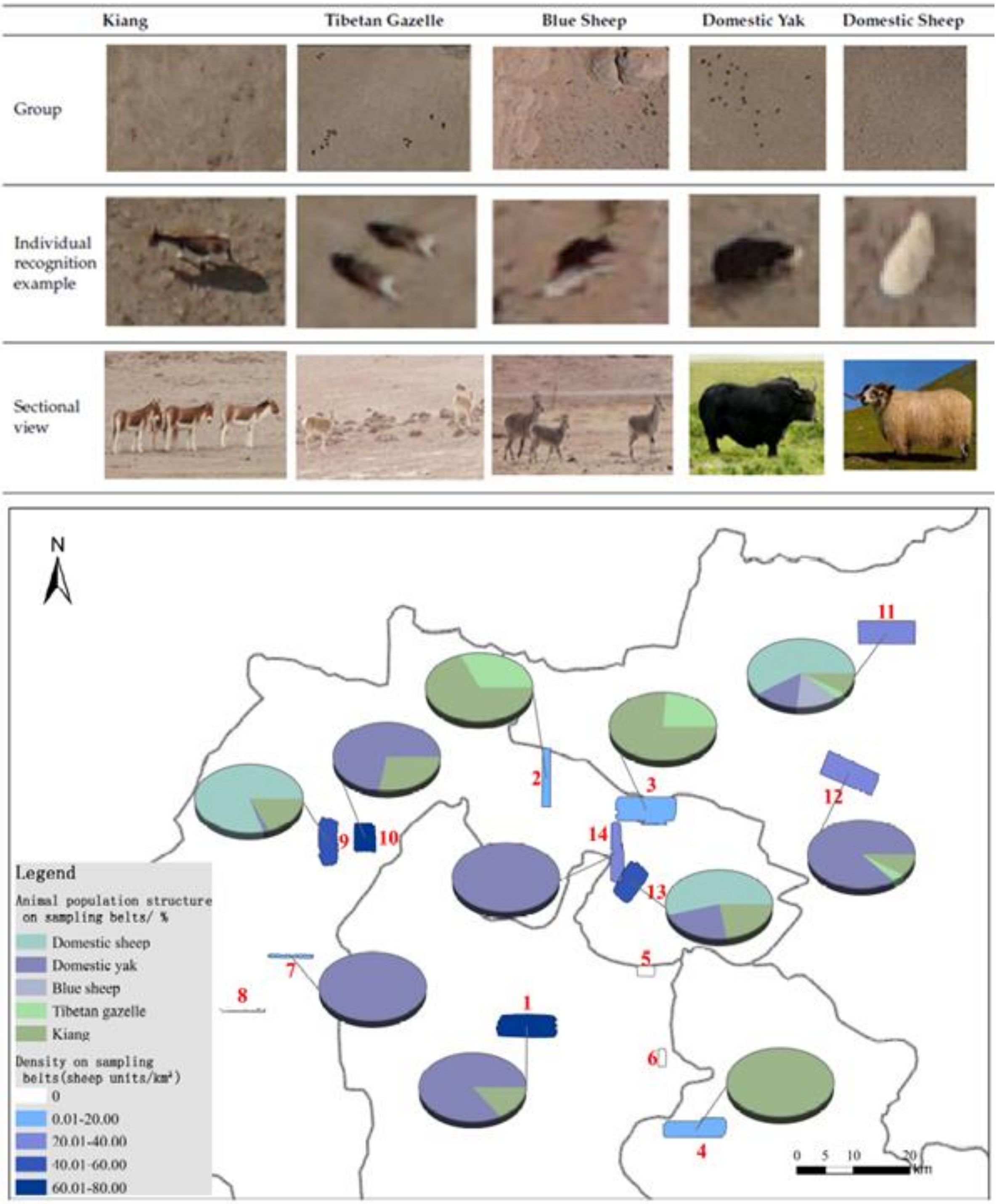

Figure 6. An example of the process of using UAVs to produce population estimates of large wild herbivores (Kiang, Tibetan gazelle, blue sheep, domestic yak and domestic sheep) in Maduo County in China from Guo *et al.* (2018). The top photographs demonstrate the types of images retrieved from the UAV next to references images of the animals. In the bottom map, the dark and light blue rectangles indicate the flight path taken by the UAV and the pie charts represent the estimated densities for different species.

Indirect measurements of wildlife population change can be derived from EO by gathering data on the habitats or conditions that are needed for those animals. These data are often used as part of species distribution modelling to predict where there is suitable habitat for that animal. For example, with an animal that is a forest specialist, measures of tree or forest cover (which can be derived from EO) are likely to be important factors in predicting where that species is found. Table 4 details a range of these types of measures (listed as “habitat suitability” under the proxy column) taken from a review of the potential for EO to be used for monitoring ecosystem functions (Pettorelli *et al.* 2018).

4.2 Wildlife management

This initial search did not bring up examples of how EO could be used to monitor wildlife management practices. There may be opportunities to use EO for indirect measures of wildlife management, for example linked to land cover change. This could be an area to explore further if additional resources become available.

4.3 Wildlife moved for hunting

The EO examples presented for detecting wildlife moved for hunting are indirect measures of human population growth, human activity (logging and fires) and human movement (expansion of roads). These measures can be detected in some way using EO, detailed in Table 4.

4.4 Exposure

Detecting exposure to wildlife (at wet markets, from subsistence hunting, ecotourism and via livestock) will be difficult using EO. This could be an area to explore further if additional resources become available.

Table 4. Wildlife drivers for EIDs, proxies that can be derived from Earth Observation data, satellites and sensors that provide appropriate data, data products available (if applicable) and applied examples. Colours indicate how accessible the EO data are: green (data product available for free), orange (data product available for a cost), red (data product not available), white (not assessed).

Driver	Proxy	Data product	Satellite (sensor) / EO	Spatial coverage	Temporal coverage	Examples
Wildlife population change	Large mammal abundance estimate		Unmanned Aerial Vehicle (UAV)	Determined by accessibility and aviation protocols. Spatial cover limited by data collection over a small area (e.g. a few kms per flight)		See Christie *et al.* (2016) for a review of studies estimating population size and other metrics. Animals include sperm whales, walrus, sea turtles, penguins, sandhill crane, flamingos, beaver, elephant, orangutans, and riverine fish habitat mapping.
	Nocturnal mammal abundance estimate		UAV with thermal cameras			Potvin and Breton (2005) used UAVs with thermal cameras to count deer in a wooded area with variable levels of accuracy (89% and 54% of deer located in two study areas).
	Indirect signs e.g. burrow counts	Medium to low resolution satellite imagery available from a range of sources.	GeoEye- (3/15), WorldView-1/2/3/4 (7/15), Quickbird-2 (3/15), IKONOS (1/15).	Regional to global depending on the satellite	0.31-1.2m depending on the satellite	Wang *et al.* (2019) reviewed the use of medium-low resolution satellites to detect fecal counts, food remove and burrow counts.
	Habitat suitability - landcover	ESA global land cover maps	ENVISAT (MERIS); SPOT (HRV, HRVIR, HRG)	Global 300m	1992-2015 yearly	Proxies, satellites and data products are taken from Pettorelli *et al.* 2018.

Driver	Proxy	Data product	Satellite (sensor) / EO	Spatial coverage	Temporal coverage	Examples
		MODIS Land Cover Type	Terra/Aqua (MODIS)	Global 500m	2001-2019 yearly	
	Habitat suitability – forest cover	Landsat Global Forest Cover Change	Landsat (TM, ETM+, OLI)	Global 10 x 10 degree	2000-2019 yearly	
		MODIS Land Cover Type	*See above.*			
	Habitat suitability – tree cover	MODIS Vegetation Continuous Fields	Terra/Aqua (MODIS)	Global 250m	2000-2020 yearly	
		Landsat Tree Cover Continuous Fields	Landsat (TM, ETM+, OLI)	Global 30m	These years 2000, 2005, 2010, 2015	
	Habitat suitability – water bodies	MODIS Water Mask	Terra/Aqua (MODIS)	Global 250m	2000-2015 yearly	
	Habitat suitability – inland water dynamics	Global Surface Water	Landsat (TM, ETM+)	Global 30m	1984-2019 Monthly and yearly	
	Habitat suitability – sea ice	Sea Ice Concentration (from Nimbus-7 and DMSP)	Nimbus-7 (SMMR) &	Global 25m	1978-2019 yearly	

Driver	Proxy	Data product	Satellite (sensor) / EO	Spatial coverage	Temporal coverage	Examples
			DMSP (SSM/I, SSMIS)			
		GRACE Monthly surface mass changes	GRACE (KBR)			
		Cryosat ice thickness	Cryosat (SIRAL)	Global 5400km	2010-present weekly	
	Habitat suitability – glaciers	GLIMS	Terra (ASTER)		1850-2018	
	Habitat suitability – salinity	SMOS salinity	SMOS (MIRAS)			
		Aquarius sea surface salinity	SAC-D (Aquarius)	Global 1 degree	2011-2015 Weekly, monthly	
	Habitat suitability – albedo	MODIS Surface Albedo product	Terra/Aqua (MODIS	Global 500m	2000-present daily	
	Habitat suitability – soil moisture	Soil moisture Product	SMAP (SMAP Radiometer)			
		ESA CCI Soil Moisture	Multiple, including ERS-1/2, Metop,	Global 0.25 degrees	1978- 2019 Daily	

Driver	Proxy	Data product	Satellite (sensor) / EO	Spatial coverage	Temporal coverage	Examples
			DMSP(SSM/I), TRMM(TMI)			
	Habitat suitability – SRS-based primary productivity estimates	MODIS Chlorophyll a	Terra/Aqua (MODIS)			
		MODIS Gross Primary Production		Global 500m	2002-present Multi-day	
		MODIS Net Primary Production		Global 500m	2002-present yearly	
	Habitat suitability – sea surface temperature	MODIS Sea Surface temperature	Terra/Aqua (MODIS)	Global 4km	2000-present 8 day	
Wildlife management practices						
Wildlife moved for hunting	Human population change	*See the previous section under human population change.*				Dupain *et al.* (2011) used LandScan data on human density and found this to be highly correlated with bushmeat harvests in the Congo.
	Human accessibility – roads, transport		(Level 3A) RapidEye satellite imagery	Global Dependant on product	Dependent on product 2009/14-present	Kearney *et al.* (2020) trained RapidEye satellite imagery with convolutional neural networks to identify roads in Canada.

Driver	Proxy	Data product	Satellite (sensor) / EO	Spatial coverage	Temporal coverage	Examples
				3-5m	Daily	
		Incorporates imagery and data products from a range of satellites.	gROADS	Global map scale of ~1:1m	One dataset for 1980-2010	
	Logging activity	*Many satellites and data products.*				Hansen *et al.* (2013) detected yearly forest cover change at a 30m resolution using Landsat satellites.
			UAV	Determined by accessibility and aviation protocols. Spatial cover limited by data collection over a small area (e.g. a few kms per flight)		Paneque-Galvez *et al.* (2014) reviewed the feasibility for using UAVs to detect illegal logging in tropical areas.
	Human activity – number of fires	Active fire data (MCD14DL)	Aqua & Terra (MODIS)	Global, 1km	2000- present	
		Active fire product (VNP14IMGTDL_NRT and VJ114IMGTDL_NRT)	Suomi NPP (VIIRS)	Global, 375m	2012- present	
Exposure to wildlife at wet markets						
Exposure to wildlife – subsistence hunting						

Driver	Proxy	Data product	Satellite (sensor) / EO	Spatial coverage	Temporal coverage	Examples
Exposure to wildlife – ecotourism						
Exposure to wildlife viruses directly via livestock						

5 Livestock drivers

Data on livestock drivers was identified as important for informing EIDs, specifically around **livestock population change**, **livestock management practices**, **movement of wildlife**, **exposure to livestock at wet markets**, **exposure to livestock ticks** and **butchering of livestock**.

5.1 Livestock population change

Like wildlife population change, it is possible to get both direct and indirect measure of livestock population change from EO. One source of direct measures is from UAVs (Figure 8i) and in some cases it may be possible to get direct measures of livestock population change from satellite imagery (Figure 8ii) although this is likely to be suitable only for very large animals and will have high error rates.

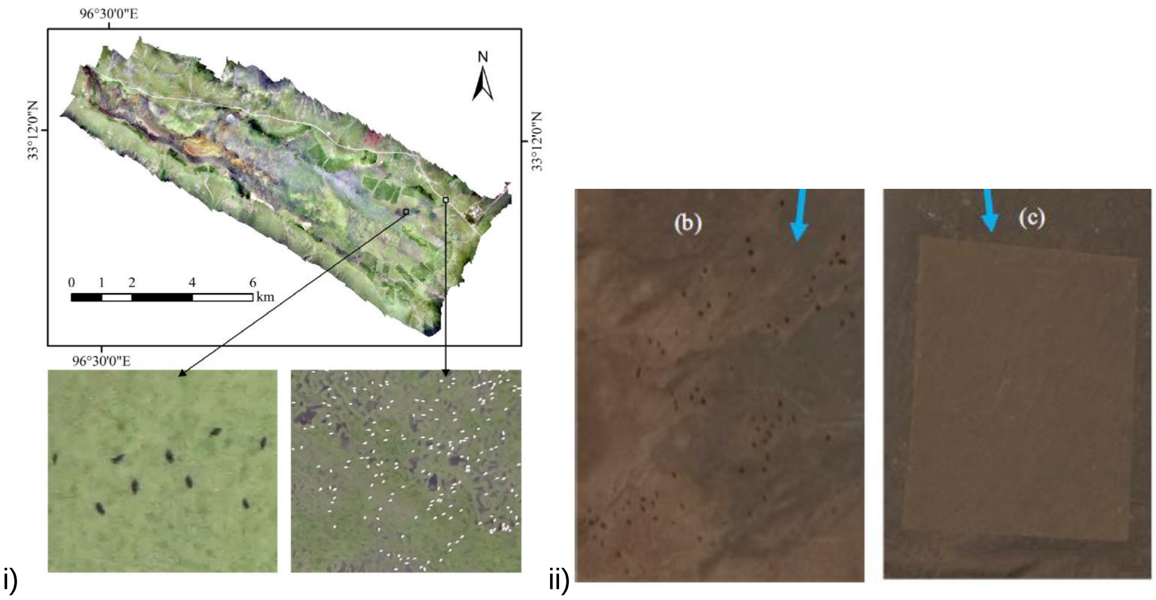

Figure 7. A comparison of UAVs and satellite imagery to identifying yaks and sheep in China. i) Imagery produced using UAVs with yaks (bottom left) and sheep (bottom right) both visible. ii) Satellite imagery where yaks are visible (b) but sheep are not (c). The field boundaries that sheep were kept in were visible in the satellite imagery (c). Images are taken from Wang *et al.* 2020b.

There have explorations of using indices that you can derive from EO like NDVI as proxies for grazing (with the assumption that grazed areas will have shorter vegetation and therefore lower NDVI values than ungrazed areas). Some of these explorations with NDVI have not been very successful (e.g. see Olsen *et al*. 2015) however there are promising examples with indices such as LAI (Leave Area Index, Wang *et al.* 2019) and commercially available applications of EO in the agricultural sector.

Another way that you could use EO as an indirect measure of livestock population change is by using modelling approaches to estimate pastureland. For example, Ramankutty *et al.* (2008) took data from two sources of satellite imagery and modelled a global estimate of pastureland for 2000 (Figure 9). This data has not been reproduced for other years.

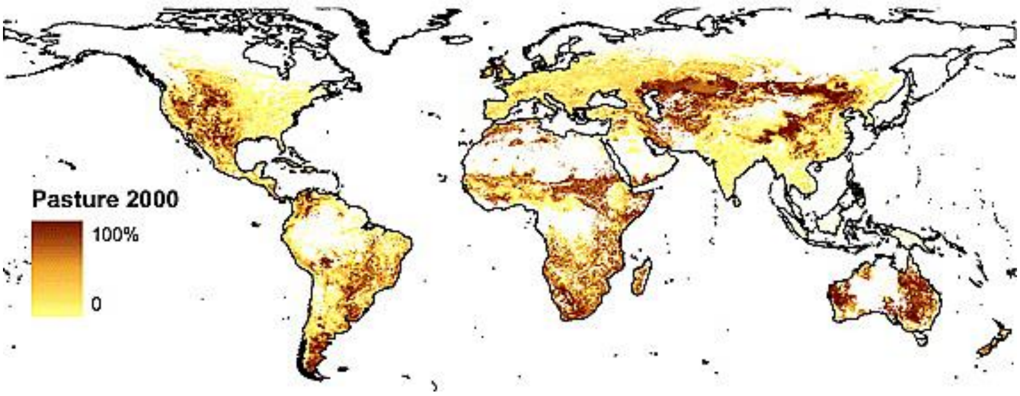

Figure 8. Global estimates of pastureland for the year 2000 (Ramankutty *et al.* 2008).

5.2 Livestock management

This initial search did not bring up examples of how EO could be used to monitor livestock management practices. This could be an area to explore further if additional resources become available.

5.3 Exposure

Detecting exposure to livestock (at wet markets and for livestock ticks) will be difficult using EO. This could be an area to explore further if additional resources become available.

5.4 Butchering of livestock

This initial search did not bring up examples of how EO could be used to the butchering of livestock and it is unlikely that EO will be able to help with these data needs.

Table 5. Livestock drivers for EIDs, proxies that can be derived from Earth Observation data, satellites and sensors that provide appropriate data, data products available (if applicable) and applied examples. The acronyms in the table are expanded here: Modetate Resolution Imaging Spectroradiometer (MODIS); Normalised Difference Vegetation Index (NDVI); Satellite Pour l'Observation de la Terre (SPOT); Socioeconomic Data and Applications Center (SEDAC). Colours indicate how accessible the EO data are: green (data product available for free), orange (data product available for a cost), red (data product not available), white (not assessed).

<table>
<tr><th>Driver</th><th>Proxy</th><th>Data product</th><th>Satellite (sensor) / EO</th><th>Spatial coverage</th><th>Temporal coverage</th><th>Examples</th></tr>
<tr><td rowspan="6">Livestock population change</td><td rowspan="2">Large mammal abundance estimate</td><td></td><td>WorldView-2</td><td>Global

<0.46m</td><td>2009-present

1-2 days</td><td>Wang et al. (2020b) identified dark dots from satellite imagery that were identifiable as yaks (2.5m long by 0.5-1m wide, in groups of >3 dots). It was not possible to identify sheep.</td></tr>
<tr><td colspan="4" rowspan="3">For the details on these proxies, see the Table 2 in the section on wildlife drivers.</td><td rowspan="2">Mulero-Pazmany et al. (2015) compared UAVs with GPS-GSM collars for counting and locating free-ranging cattle

Wang et al. (2020b) identified sheep and yaks using UAVs but could not identify abundant black-necked cranes or other birds.</td></tr>
<tr><td>Nocturnal mammal abundance estimate</td></tr>
<tr><td>Indirect signs e.g. burrow counts</td><td></td></tr>
<tr><td rowspan="2">Agricultural/ pastural land</td><td>Global Agricultural Lands from SEDAC</td><td>MODIS and SPOT</td><td>Global</td><td>2000

1 year</td><td>The methodology describing the production of this data product is found in Ramankutty et al. 2008.</td></tr>
<tr><td>MOD13Q1

(NDVI)</td><td>MODIS</td><td>Global

250m</td><td>2000-present

16 days</td><td>Olsen et al. (2015) compared NDVI metrics with measured volumes of end of season standing biomass and found that grazing signals were not clearly separated from weather effects.</td></tr>
</table>

Driver	Proxy	Data product	Satellite (sensor) / EO	Spatial coverage	Temporal coverage	Examples
Movement of wildlife	*See the section on wildlife for example proxies of this.*					
Exposure to livestock at wet markets						
Exposure to livestock ticks						
Butchering of livestock						

6 Composition of landscape and land use

Data on the composition of landscape and land use was identified as important for informing EIDs, specifically around **fragmentation of the landscape and land use**, and **land use and farm management**. EO is very well suited for classifying land cover which when used in a time series can give measure of land use. There will be many suitable land cover products available which can be used for this application (e.g. see this review by the Living Wales programme). As this area of work is well established, the following gives only a few illustrative examples.

6.1 Classifying land cover from EO

Producing land cover maps from EO images involves classification of images that is either supervised (human-guided) or unsupervised (calculated by computer software). These methods require training datasets of known examples (in space and time) of land cover types. The spatial and land cover class accuracy of these products varies with scale, the appropriateness of the training data and the land class types used. A landscape scale mapping project with a lot of quality training data and clear land class types will likely produce a more accurate land class map than a global mapping project with little training data. Examples of mapping projects at different spatial scales are: the Living England project by Natural England (landscape scale / small country scale), CORINE by the Copernicus Land Monitoring Service (a regional map which covers continental Europe), and the Land Cover product by the Copernicus Global Land Service (a global dataset). These types of mapping products can be used to extract information on fragmentation of the landscape and land use, and land use and farm management.

6.2 Fragmentation of landscape and land use

There are many ways to extract information about fragmentation from EO. This report gives a light touch to give examples of this as this is a well-established field. Figure 10 gives a visual example of how this might be carried out.

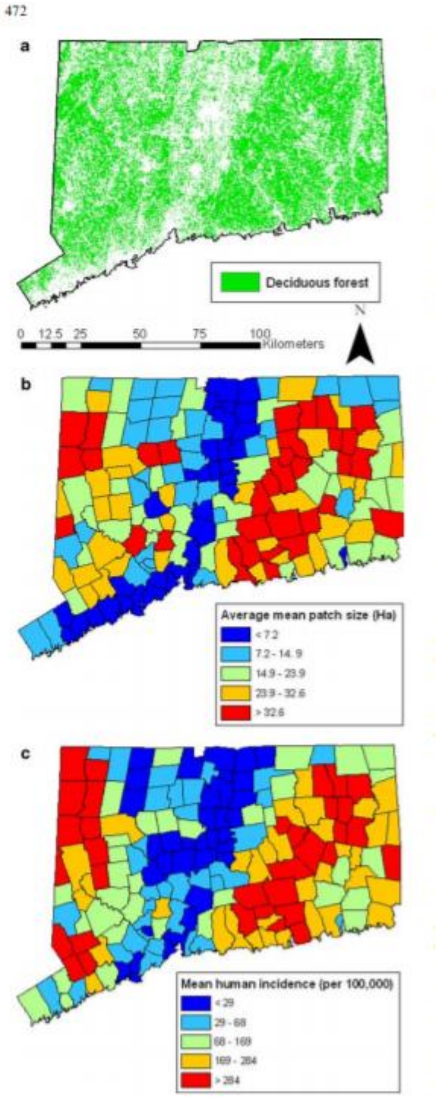

Figure 10. EO was used to identify forest cover (a), which was analysed using fragmentation software (b) and correlated with the incidences of Lyme disease in humans (c). Taken from Brownstein *et al.* (2005).

6.3 Land use and farm management

There are many EO products that can produce information about land use and more frequently now habitat (e.g. Living Maps are now being produce by the UK's countries for detailed habitat maps derived from EO using Sentinel data). For the purposes of this report, the proxies, satellites and data products given are taken from another review, Kotchi *et al.* (2019).

Table 6. Composition of landscape and land use drivers for EIDs, proxies that can be derived from Earth Observation data, satellites and sensors that provide appropriate data and applied examples. Satellite data have been used to map the earth's surface and is well-established with the sensor's listed below (other sensors are available and being launched all the time with this capability at varying scales and accessibility). **No data products were included in this table so the traffic light system for scoring data accessibility was not used.** The information for land use proxies of land cover, soil type vegetation type and vegetation quantity are taken from Kotchi *et al*. 2019.

Driver	Proxy	Satellite (sensor) / EO	Spatial coverage	Temporal coverage	Examples
Fragmentation of landscape and land use	*Analyses such as calculating patch size are applied to the land use products described below.*				Brownstein *et al.* (2005) calculated forest fragmentation from EO data sources to predict local occurrences of Lyme disease.
Land use and farm management	Land cover	SPOT-4 Vegetation instrument	20m	1998 – 2013 1 day	Leblond *et al.* (2007) used SPOT-4 measurements to classify 14 landscape categories and associate these with mosquito, bird and horse abundances for West Nile disease
		Landsat-5 (TM)	30-120m	16 days	
		Landsat-7 (ETM+)	15-60m	16 days	
		Landsat-8 (OLI)	15-30m	16 days	
		NOAA 15-19 (AVHRR/3)	1.1km	0.5 days	
		Sentinel-1 (C-SAR)	10-60m	12 days	
		Sentinel-2 (MSI)	Global 300m (100m for the data product)	5 days (Annual for the data product, 2015-present)	
		Sentinel-3 (OLCI)	300m	2 days	
		Terra, Aqua (MODIS)	250-1000m	5 min	

Driver	Proxy	Satellite (sensor) / EO	Spatial coverage	Temporal coverage	Examples
			(500m-1km for data product)	(Yearly for data product)	
	Soil type	Landsat-5 (TM)	30-120m	16 days	Forkour *et al.* (2017) used RapidEye and Landsat data with analysed soil samples to map soil properties (sand, silt clay, cation exchange capacity, soil organic carbon and nitrogen) in Burkina Faso. Images of bare soil (during ploughing or early crop stages) were classified more accurately than at other times.
		Landsat-7 (ETM+)	15-60m	16 days	
		Landsat-8 (OLI)	15-30m	16 days	
		Sentinel-2 (MSI)	300m	5 days	
		Terra	15-90m	5 days	
		Terra, Aqua	250-1000m	5 min	
	Vegetation type	Landsat-5 (TM)	30-120m	16 days	
		Landsat-7 (ETM+)	15-60m	16 days	
		Landsat-8 (OLI)	15-30m	16 days	
		Sentinel-1 (C-SAR)	10-60m	12 days	
		Sentinel-2 (MSI)	300m	5 days	
		Terra, Aqua	250-1000m	5 min	
	Vegetation quantity	Landsat-5 (TM)	30-120m	16 days	
		Landsat-7 (ETM+)	15-60m	16 days	
		Landsat-8 (OLI)	15-30m	16 days	

Driver	Proxy	Satellite (sensor) / EO	Spatial coverage	Temporal coverage	Examples
		MSG (SEVIRI)	1-48km	15 min	
		NOAA 15-19 (AVHRR/3)	1.1km	0.5 days	
		Sentinel-1 (C-SAR)	10-60m	12 days	
		Sentinel-2 (MSI)	300m	5 days	
		Sentinel-3 (OLCI)	300m	2 days	
		Sentinel-3 (SLSTR)	500-1000m	1-4 days	
		SNPP (VIIRS)	375-750m	6 min	
		Terra	15-90m	5 days	
		Terra, Aqua	250-1000m	5 min	
		LiDAR			

7 Climate / weather

Data on climate/weather was identified as important for the spread and establishment of EIDs, specifically around **climate change over time**, **climate change range expansion**, and **weather patterns (seasonal).** EO datasets play a large role in climate modelling and as this area of work is large, the following gives only a few illustrative examples. There are also overlaps in this section with the final section on zoological/virological drivers as EO derived climate variables are often used to predict vector and virus distributions. It is important to note that many ecological niche models for vectors and viruses use weather data that does not use EO and instead models values using observed values (e.g. HadUK-Grid from the Met Office for a UK scale or WorldClim at a global scale).

The Global Climate Observing System (GCOS) aims to provide comprehensive information on the climate system which has led to the formation of Essential Climate Variables (ECV). The GCOS has set out requirements for EO to meet these needs (GCOS 2011) which are starting to be met through programmes such as the Copernicus Land Service which aims to produce EO derived data products for some of the ECVs.

An example of how EO derived climate data can be applied for horizon scanning for EIDs can be seen in Anyamba *et al.* (2019) where EO was used to gather data on climactic variables related to the 2015-16 El Niño event (Figure 11). These data were correlated with global disease outbreaks (e.g. chikungunya, hantavirus, Rift Valley fever, cholera, plague and Zika). The diseases and environmental variables were found to be related and a system was developed to provide monthly or quarterly early warning alerts for disease outbreaks in different regions.

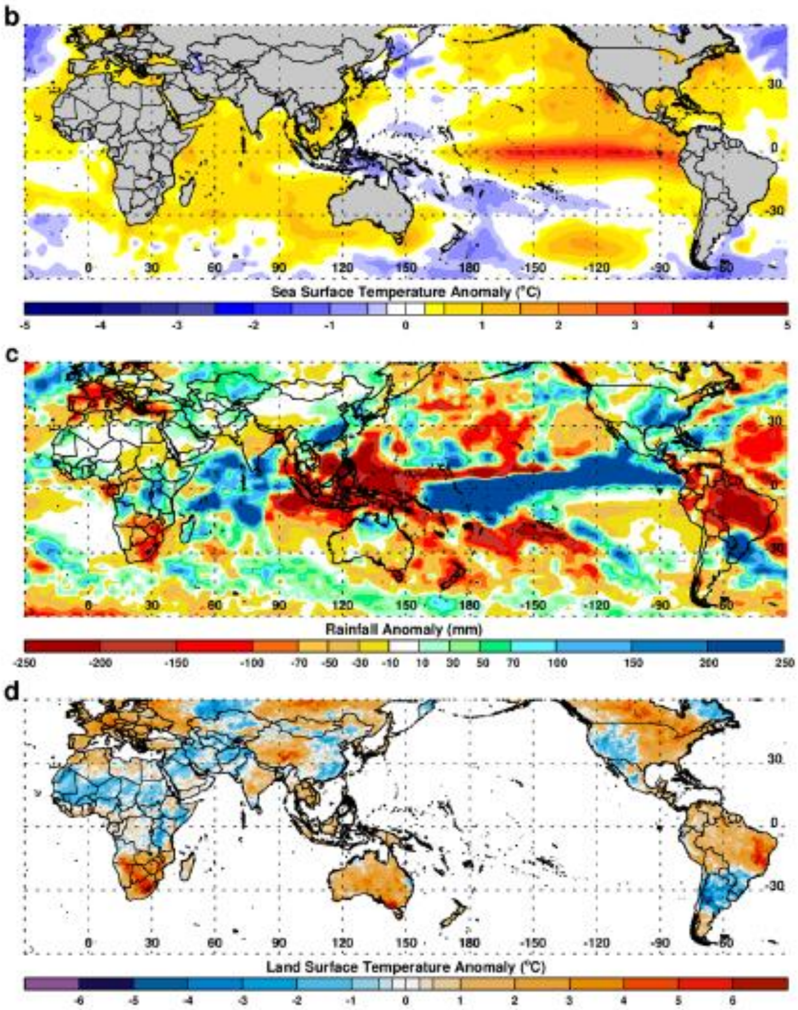

Figure 11. EO data on b) Sea Surface Temperature, c) Rainfall and d) Land Surface Temperature anomalies related to the 2015-16 El Niño event (Anyamba *et al.* 2019).

Table 7. Climate / weather drivers for EIDs, proxies that can be derived from Earth Observation data, satellites and sensors that provide appropriate data, data products available (if applicable) and applied examples. Satellite data have been used to derive climate data and incorporate into climate models. It is well-established with the sensor's listed below (other sensors are available and being launched all the time with this capability at varying scales and accessibility). Colours indicate how accessible the EO data are: green (data product available for free), orange (data product available for a cost), red (data product not available), white (not assessed). **No data products were included for the examples taken from Kotchi *et al*. 2019 for climate change over time so the traffic light system for scoring data accessibility was not used for those examples. Where a data product lists Living Wales, there is a link which to a webpage where there may be several potential datasets which have not been evaluated with the traffic light system.**

Driver	Proxy	Data product	Satellite (sensor) / EO	Spatial coverage	Temporal coverage	Examples
Climate change over time	Snow cover depth		DMSP (SSM/I)	13-69km	1 day	Taken from Kotchi *et al.* (2019) who reviewed the use of Earth observation to inform risk assessments and mapping related to climate change and infectious diseases.
			GCOM-W1 (AMSR-2)	3-62 km	1 day	
			Landsat-5 (TM)	30-120m	16 days	
			Landsat-7 (ETM+)	15-60m	16 days	
			Landsat-8 (OLI)	15-30m	16 days	
			NOAA 15-19 (AVHRR/3)	1.1km	0.5 days	
			Sentinel-1 (C-SAR)	10-60m	12 days	
			Sentinel-2 (MSI)	300m	5 days	
			Sentinel-3 (SLSTR)	500-1000m	1-4 days	
			SNPP (VIIRS)	375-750m	6 min	
			Terra	15-90m	5 days	
			Terra, Aqua	250-1000m	5 min	

Driver	Proxy	Data product	Satellite (sensor) / EO	Spatial coverage	Temporal coverage	Examples
		Living Wales catalogue of products for Snow Depth				
	Snow cover extent	Copernicus Global Land Service Snow Cover Extent	(MODIS)	Continental Europe 500m	March 2017-present Within 1 day	Snow cover is specified as Essential Climate Variable (ECV) by the Global Climate Observing System (GCOS).
	Water quality		GCOM-W1 (AMSR-2)	3-62km	1 day	Taken from Kotchi *et al.* (2019).
			Sentinel-3 (OLCI)	300m	2 days	
			SMAP (MWR)	40km	1.5 days	
			Terra, Aqua	250-1000m	5 min	
			Sentinel-2			
			Landsat			
	Surface humidity		Landsat-5 (TM)	30-120m	16 days	Taken from Kotchi *et al.* (2019).
			Landsat-7 (ETM+)	15-60m	16 days	
			MSG (SEVIRI)	1-48km	15 min	
			NOAA 15-19 (AVHRR/3)	1.1km	0.5 days	
			SMAP (MWR)	40km	1.5 days	

Driver	Proxy	Data product	Satellite (sensor) / EO	Spatial coverage	Temporal coverage	Examples
			SNNP (ATMS)	16-75km	0.5 days	
			SNPP (VIIRS)	375-750m	6 min	
			Terra, Aqua	250-1000m	5 min	
	Surface temperature		Aqua (AIRS)	2.3-41km	0.5 days	Taken from Kotchi *et al.* (2019).
			GPM (GMI)	4-32km	1-2 hours	
			Landsat-5 (TM)	30-120m	16 days	
			Landsat-7 (ETM+)	15-60m	16 days	
			Landsat-8 (TIRS)	100m	8 days	
			MSG (SEVIRI)	1-48km	15 min	
			NOAA 15-19 (AVHRR/3)	1.1km	0.5 days	
			Sentinel-3 (SLSTR)	500-1000m	1-4 days	
			SNPP (VIIRS)	375-750m	6 min	
			Terra	15-90m	5 days	
			Terra, Aqua	250-1000m	5 min	
		Copernicus Global Land Service Land Surface Temperature	Constellation of geostationary (GEO) satellites: Meteosat Second Generation, Meteosat Second	Global 5km	Jan 2021 – present, hourly,	In production.

Driver	Proxy	Data product	Satellite (sensor) / EO	Spatial coverage	Temporal coverage	Examples
			Generation Indian Ocean Data Coverage, Geostationary Operational Environmental Satellite, Himawari		within 4 hours	
	Air temperature		Aqua (AIRS)	2.3-41km	0.5 days	Taken from Kotchi *et al.* (2019).
			SNNP (ATMS)	16-75km	0.5 days	
			Terra, Aqua	250-1000m	5 min	
	Water vapour		DMSP (SSM/I)	13-69km	1 day	Taken from Kotchi *et al.* (2019).
			GCOM-W1 (AMSR-2)	3-62 km	1 day	
			GPM (GMI)	4-32km	1-2 hours	
			Landsat-8 (TIRS)	100m	8 days	
			MSG (SEVIRI)	1-48km	15 min	
			NOAA 15-19 (AVHRR/3)	1.1km	0.5 days	
			SNPP (VIIRS)	375-750m	6 min	
			Terra	15-90m	5 days	
			Terra, Aqua	250-1000m	5 min	
	Precipitation		DMSP (SSM/I)	13-69km	1 day	Taken from Kotchi *et al.* (2019).

Driver	Proxy	Data product	Satellite (sensor) / EO	Spatial coverage	Temporal coverage	Examples
			GCOM-W1 (AMSR-2)	3-62 km	1 day	
			GPM (DPR)	5km	1-2 hours	
			GPM (GMI)	4-32km	1-2 hours	
			MSG (SEVIRI)	1-48km	15 min	
Climate change range expansion	*EO plays an important role in climate modelling.*					
Weather patterns (seasonal)	Sea-surface temperature (SST)	High-resolution Blended Analysis of Daily SST and Ice	NOAA/CPC (AVHRR)	Global ¼ degree	Sept 1981 - present	Anyamba *et al. (*2009) calculated monthly & seasonal anomalies (difference to the mean in degrees Celsius) for Rift Valley fever outbreak Anyamba *et al.* (2019) used SST to explore the impact of El Nino on global disease outbreaks. Linthicum *et al.* (1999) used SST anomalies for Rift Valley fever outbreak
	Outgoing Longwave Radiation (linked to El Niño)	NOAA Interpolated Outgoing Longwave Radiation (OLR)	NOAA/CPC (AVHRR)	Global 2.5 x 2.5 degrees	June 1974 - present	Anyamba *et al. (*2009) calculated monthly anomalies for Rift Valley fever outbreak

Driver	Proxy	Data product	Satellite (sensor) / EO	Spatial coverage	Temporal coverage	Examples
	Rainfall	Africa Rainfall Climatology Version 2.0 (ARC2)	NOAA/CPC Special Sensor Microwave/ Imager, Advanced Microwave Sounding Unit & Infrared bands of METEOSAT platforms	Africa 40N- -40S, -20W – 55E 1 degree	1st Jan 1983 - present	Anyamba *et al.* (2009) calculated monthly total, seasonal total and corresponding anomalies for Rift Valley fever outbreak. Anyamba *et al.* (2019) used rainfall to explore the impact of El Nino on global disease outbreaks.
	Water seasonality	Living Wales catalogue of products for Water Seasonality				

8 Zoological / virological

Data on zoological/ virological drivers was identified as important for informing EIDs, specifically around **monitoring invasive species**, **change in abundance or range of reservoirs and vectors**, and **adaptation to new environments by vectors or viruses**. The literature has many examples of researchers using EO to understand the relationship of the changing environment to disease outbreaks. For instance, it is well established that green vegetation (NDVI) and precipitation are linked to some insect pests and vectors like mosquitoes and locusts, which are commonly derived variables from EO (see Pettorelli *et al.* 2011 for a review on the use of NDVI in ecological studies). For illustrative examples of how EO can be used to gather data on zoological/ virological drivers, refer to the case study in section 2.

Table 8. Zoological / virological drivers for EID, proxies that can be derived from Earth Observation data, satellites and sensors that provide appropriate data, data products available (if applicable) and applied examples. For many of the products that are listed, these can be produced using several satellites and sensors. The examples given here have been taken from research papers demonstrating their use. Colours indicate how accessible the EO data are: green (data product available for free), orange (data product available for a cost), red (data product not available), white (not assessed).

Driver	Proxy	Data product	Satellite (sensor) / EO	Spatial coverage	Temporal coverage	Examples
Monitoring of Invasive species	Heat signals	NA	Thermal cameras	Dependant on the application.		Kennedy *et al*. (2018) used thermal imaging to detect Asian hornets.
	Habitat suitability	*See habitat suitability within the wildlife population section.*				
Change in abundance / range of reservoirs and vectors	Normalised Difference Vegetation (NDVI)		NOAA/CPC AVHRR	Global 4km	1981-present	Anyamba *et al. (*2009) used historic NDVI values and disease outbreak locations to map the risk of outbreaks for Rift Valley fever. Anyamba *et al.* (2019) used NDVI to explore the impact of El Nino on global disease outbreaks. Batallan *et al.* (2015) used NDVI as a proxy for habitat presence to predict mosquito dynamics. Brooker *et al*. (2001) used LST to predict the infection rate of urinary schistosomiasis. Estrada-Peña *et al.* (2007) calculated 10-day average NDVI values and compared these with an average across the previous year to predict the beginning of Crimean-Congo haemorrhagic fever (CCHF) season in Turkey (vector: *Hyalomma* vector ticks). Linthicum *et al.* (1999) used abnormally high levels of NDVI to detect abnormally high rainfall and predict Rift Valley fever outbreak.
			SPOT-4	Global 1km	1998 – 2013 daily	
			SPOT-5	Global 1km	daily	

Driver	Proxy	Data product	Satellite (sensor) / EO	Spatial coverage	Temporal coverage	Examples
						Stensgaard *et al.* (2005) used NDVI in modelling the host snails for *Schistosoma mansoni*.
	Enhanced Vegetation Index (EVI)	MCD43B4	Terra (MODIS)	1km	Feb 2000 – March 2017	Pigott *et al.* (2014) calculated the mean and range of the values in a 5x5km area (spatial heterogeneity) for a species distribution model for the Ebola virus.
	Normalized Difference Water Index (NDWI Max Feeters)		SPOT-5	Global 1km	2002 – 2015, revisit= 2-3 days	Machault *et al.* (2012) used NDVI for risk mapping *Anopheles* larval habitats as malaria vectors. Batallan *et al.* (2015) used NDWI to predict mosquito dynamics.
	Modified NDWI Mac Feeters Index (MNDWI)		SPOT-5	Global 1km	2002 – 2015, revisit= 2-3 days	Machault *et al.* (2012) used MNDVI for risk mapping *Anopheles* larval habitats as malaria vectors.
	Brightness Index (BI)		SPOT-5	Global 1km	2002 – 2015, revisit= 2-3 days	Machault *et al.* (2012) used BI for risk mapping *Anopheles* larval habitats as malaria vectors.
	Precipitation – ARC	*See the previous section on climate change.*				Anyamba *et al. (*2009) used historic ARC values and disease outbreak locations to map the risk of outbreaks for Rift Valley fever Anyamba *et al.* (2019) used rainfall to explore the impact of El Nino on global disease outbreaks.

Driver	Proxy	Data product	Satellite (sensor) / EO	Spatial coverage	Temporal coverage	Examples
	Land Surface Temperature (LST)	MOD11A2	Terra (MODIS)	1km	Feb 2000 - Present	Anyamba *et al.* (2019) used LST to explore the impact of El Nino on global disease outbreaks Brooker *et al*. (2001) used LST to predict the infection rate of urinary schistosomiasis. Pigott *et al.* (2014) used daytime LST, nighttime LST and the mean potential evapotranspiration for a species distribution model for the Ebola virus Machault *et al.* (2012) used average values across 3 decades for risk mapping *Anopheles* larval habitats as malaria vectors Rizzoli *et al.* (2007) calculated autumnal temperature decline (August-October) relative to the annual maximum of the monthly LST level in midsummer to predict the following spring activity of *Ixodes Ricinus* for tick-borne encephalitis (TBE). Stensgaard *et al.* (2005) used LST in modelling the host snails for *Schistosoma mansoni*.
			NOAA (AVHRR)	Global 4km	1981-present	
	Elevation	Near-global Digital Elevation Models (DEMs),	Shuttle radar topography mission (SRTM)	Global 30 arc-second	NA	Brooker *et al*. (2001) used DEM to predict the infection rate of urinary schistosomiasis. Pigott *et al.* (2014) used elevation as part of a species distribution model for the Ebola virus

Driver	Proxy	Data product	Satellite (sensor) / EO	Spatial coverage	Temporal coverage	Examples
		ORNL DAAC				Machault *et al.* (2012) used elevation for risk mapping *Anopheles* larval habitats as malaria vectors
Adaptation to new environment (vectors / virus)						

9 Conclusions

This report reviews whether EO could be useful in horizon scanning for EIDs. There are numerous potentially useful EO datasets that could be applied in this context which are summarised in this report, including a case study and examples of how EO could be applied to horizon scanning EIDs and links to data sources within the tables. This report is intended as a guide and reference; however, researchers will need to assess the suitability of EO for their particular system of interest. Advice can be sought for specific applications of EO through networks such as the Defra EO Centre of Excellence or from the data providers (found through the links in the table).

A strength of EO data is that the spatial coverage is often large (e.g. global, as indicated in the tables). This is valuable in horizon scanning for EIDs which often needs to be carried out at large scales, for instance assessing the risk of a new disease arriving in Europe which originates in another continent. Another element of its spatial cover is the resolution. Many freely available EO datasets have coarse resolutions (e.g. 500m to kms) however this is improving, with projects such as the Copernicus programme collecting data at much finer resolutions (meters) allowing for higher resolution data products. Many commercial satellite data providers are also collecting frequent, high spatial resolution datasets at global scales, and the technology is fast moving, but these datasets come with a data access cost. These levels of resolution mean that it is more likely that EO will be useful in providing proxies rather than direct measures of vectors, hosts and other drivers of diseases.

EO was also assessed against temporal coverage. If relying solely on derived EO data products, the temporal coverage may be limited, for instance data products produced annually. However, it is often possible to extract indices or produce data products at a much higher temporal resolution (e.g. daily). This is particularly important as many of the drivers (monitoring human, wildlife and livestock population changes, landscape fragmentation) are currently dependent on data collection methods that are resource intensive, have gaps and can quickly become out of date. Another strength of EO data is that there are large collections of historic data, which is helpful in exploring and understanding past patterns of disease.

Although EO data has strengths in both spatial and temporal coverage, there is an important caveat which is that EO cannot often be used in insolation when monitoring or predicting infectious diseases. Many of the examples given in this report, use EO in conjunction with other data sources, e.g. pairing EO indices with disease outbreak cases which provide data on disease transmission and vector abundance. This research is important in developing proxies from EO, some of which are already well established such as the links between green vegetation (NDVI) and precipitation with some insect pests and vectors (mosquitos and locusts).Future work in this area could involve more in-depth reviews, particularly around some of the drivers that have potential for use of EO through proxies that were not covered in this desk study e.g. wildlife management. These could be case studies on specific diseases of interest including detailed exploration on drivers or expanded to other related themes like crop change products or animal density surfaces. This work could also inform on potential future operational use of EO datasets for monitoring EIDs.

References

Anderson, D.E. & Anderson, P.N. 1973. Population estimates by humans and machines. *Photogrammetric Engineering*, **39**, 147–54.

Anyamba, A., Chretien, J-P., Small, J., Tucker, C.J., Formenty, P.B., Richardson, J.H., Britch, S.C., Schnabel, D.C., Erickson, R.L. & Linthicum, K.J. 2009. Prediction of a Rift Valley fever outbreak. *Proceedings of the National Academy of Sciences of the United States of America*, **106**, 955-959.

Anyamba, A, Chretien, J-P, Britch, S.C., Soebiyanto, R.P., Small, J.L., Jepson, R., Forshey, B.M., Sanchez, J.L., Smith, R.D., Harris, R., Tucker, C.J., Karesh, W.B.& Linithicum, K.J. 2019. Global disease outbreaks associated with the 2015-2016 El Nino event. *Scientific Reports*, **9**, 1930.

Azar, D., Graesser, J., Engstrom, R., Comenetz, J., Leddy, R.M., Schechtman, N.G. & Andrews, T. 2010. Spatial refinement of census population distribution using remotely sensed estimates of impervious surfaces in Haiti. *International Journal of Remote Sensing*, **31**, 5635–55.

Batallán, G.P., Estallo, E.L., Flores, F.S., Sartor, P., Contigiani, M.S. & Almirón, W. R. 2015. St. Louis Encephalitis virus mosquito vectors dynamics in three different environments in relation to remotely sensed environmental conditions. *Acta Tropica*, **146**, 53–59.

Balk, D.L., Deichmann, U., Yetman, G., Pozzi, F., Hay, S.I. & Nelson, A. 2006. Determining global population distribution: methods, applications and data. *Advances in Parasitology*, **62**, 119-156.

Brooker, S., Hay, S.I., Issae, W., Hall, A., Kihamia, C.M., Lwambo, N.J.S., Wint, W., Rogers, D.J. & Bundy D.A.P. 2001. Predicting the distribution of urinary schistosomiasis in Tanzania using satellite sensor data. *Tropical Medicine and International Health*, **6**, 998–1007.

Bowden, S.E., Magori, K. & Drake J.M. 2011. Regional differences in the association between land cover and West Nile virus disease incidence in humans in the United States. *American Journal of Tropical Medicine and Hygiene*, **84**, 234–238.

Brownstein, J.S., Skelly, D.K., Holford, T.R. & Fish, D. 2005. Forest fragmentation predicts local scale heterogeneity of Lyme disease risk. *Oecologia*, **146**, 469-475.

Bustos, M.F.A. & Hall, O. Andersson, M. 2015. Nighttime lights and population changes in Europe 1992-2012. *Ambio*, **44**, 653-665.

Candeloro, L., Ippoliti, A., Iapaolo, F., Monaco, F., Morelli, D., Cuccu, R., Fronte, P., Calderara, S., Vincenzi, S., Porrello, A., D'Alterio, N., Calistri, P. & Conte, A. 2020. Predicting WNV circulation in Italy using Earth Observation data and extreme gradient boosting model. *Remote Sensing*,**12**, 3064.

Christie, K.S., Gilbert, S.L., Brown, S.L., Hatfield, M. & Hanson, L. 2016. Unmanned aircraft systems in wildlife research: Current and future applications of a transformative technology. *Frontiers in Ecology and the Environment*, **14**, 241-251.

Dupain, J., Nackoney, J., Vargas J.M., Johnson, P.J., Farfan, M.A., Bofaso, M. & Fa, J.E. 2012. Bushmeat characteristics vary with catchment conditions in a Congo market. *Biological Conservation*, **146**, 32-40.

Epp, T.Y., Waldnre, C. & Berke, O. 2011. Predictive risk mapping of West Nile virus (WNV) infection in Saskatchewan horses. *Canadian Journal of Veterinary Research*, **75**, 161-170.

Estrada-Peña, A., Vatansever, Z., Gargili, A. & Buzgan, T. 2007 An early warning system for Crimean-Congo haemorrhagic fever seasonality in Turkey based on remote sensing technology. *Geospatial Health,* **2**, 127-135.

Forkuor, G., Hounkpatin, O.K.L., Welp, G. & Thiel, M. 2017. High resolution mapping of soil properties using remote sensing variables in south-western Burkina Faso: a comparison of machine learning and multiple linear regression models. *PLoS ONE,* **12**, e0170478.

Fuller, T., Thomassen, H.A., Mulembakani, P.A., Johnston, S.C., Lloyd-Smith, J.O., Kisalu, N.K., Lutete, T.K., Blumberg, S., Fair, J.N., Wolfe, N.D., Shongo, R.L., Formenty, P., Meyer, H., Wright, L.L., Muyembe, J.-J., Buermann, W., Saatchi, S.S., Okitolonda, E., Hensley, L., Smith, T.B. & Rimoin, A.W. 2011. Using remote sensing to map the risk of human monkeypox virus in the Congo Basin. *Ecohealth*, **8**, 14-25.

GCOS. 2011. Systematic observation requirements for satellite-based products for climate 2011 update. WMO GCOS Rep. 154, 127 pp.

Greidanus, H., Alvarez, M., Santamaria, C., Thoorens, F-X., Kourti, N. & Argentieri, P. 2017. The SUMO ship detector algorithm for satellite radar images. *Remote Sensing*, **9**, 246.

Grover, A., Kumar, S. & Kumar, A. 2018. Ship detection using Sentinel-1 SAR data. *Remote Sensing and Spatial Information Sciences*, **5**, 317-324.

Guo, X., Shao, Q., Li, Y., Wang, Y., Wang, D., Liu, J., Fan, J. & Yang, F. 2018. Application of UAV remote sensing for a population census of large wild herbivores- taking the headwater region of the Yellow River as an example*. Remote Sensing*, **10**, 1041.

Hansen, M.C., Potapov, P.V., Hancher, M., Turubanova, S.A., Tyukavina, A., Thau, D., Stehman, S.V., Goetz, S.J., Loveland, R., Kommareddy, A., Egorov, A., Chini, L., Justice, C.O. & Townshend, J.R.G. 2013 High-resolution global maps of 21st-century forest cover change. *Science*, **342**, 850-853.

Hardy, A., Ettritch, G., Cross, D.E., Bunting, P., Liywalii, F., Sakala, J., Silumesii, A., Singini, D., Smith, M., Willis T. & Thomas, C. J. (2019) Automatic detection of open and vegetated water bodies using Sentinel 1 to map African malaria vector mosquito breeding habitats. *Remote Sensing*, **11**, 593.

Hay, S.I., Guerra, C.A., Tatem, A.J., Atkinson, P.M. & Snow, R.W. 2011. Urbanization, malaria transmission and disease burden in Africa. *Nature Reviews Microbiology*, **3**, 81-90.

Hay, S.I., Noor, A.M., Nelson, A. & Tatem, A.J. (2005b) The accuracy of human population maps for public health application. *Tropical Medicine & International Health*, **10**, 1073–1086.

Imhoff, M.L. & Bounoua, L. 2006. Exploring global patterns of net primary production carbon supply and demand using satellite observations and statistical data. *Journal of Geophysical Research*, **11**, D22S12.

Kearney, S.P., Coops, N.C., Sethi, S. & Stenhouse, G. 2020. Maintaining accurate, current, rural road network: an extraction and updating routine using RapidEye, participatory GIS and deep learning. *International Journal of Applied Earth Observation and Geoinformtion*, **87**, 102031.

Kennedy, P.J., Ford, S.M., Poidatz, J., Thiéry, D. & Osborne, J.L. 2018. Searching for nests of the invasive Asian hornet (*Vespa velutina*) using radiotelemetry. *Communications Biology*, **1**, 88.

Kotchi, S.O., Bouchard, C., Ludwig, A., Rees, E.E. & Brazeau, S. 2019. Using Earth observation images to inform risk assessment and mapping of climate change-related infectious diseases. *Canada Communicable Disease Report*, **45**, 133-142.

Lee, E., Mokashi, A.J., Moon, S.Y. & Kim, G.S. (2019) The maturity of Automatic Indification Systems (AIS) and its application for innovation. *Journal of Marine Science and Engineering.* **7**, 287.

Li, C., Chen, G, Luo, J., Li, S. & Ye, J. 2017. Port economics comprehensive scores for major cities in the Yangtze Valley, China using the DMSP-OLS night-time light imagery. *International Journal of Remote Sensing*, **38**, 6007–6029.

Li, X. & Zhou, Y. 2017. Urban mapping using DMSP/OLS stable night-time light: a review. *International Journal of Remote Sensing*, **38**, 6030–6046.

Liang, H., Tanikawa, H., Matsuno, Y. & Dong, L. (2014) Modeling in-use steel stock in China's buildings and civil engineering infrastructure using time-series of DMSP/OLS nighttime lights. *Remote Sensing*, **6**, 4780–4800.

Liu, H. & Weng, Q. 2012. Enhancing temporal resolution of satellite imagery for public health studies: A case study of West Nile Virus outbreak in Los Angeles in 2007. *Remote Sensing of Environment*,**117**, 57–71.

Linard, C., Gilbert, M. & Tatem, A.J. 2011. Assessing the use of global land cover data for guiding large area population distribution modelling. *GeoJournal*, **77**, 525–538.

Linthicum, K.J., Anyaba, A., Tucker, C.J., Kelley, P.W., Myers, M.F. & Peters, C.J. 1999. Climate and satellite indicators to forecast Rift Valley Fever epidemics in Kenya, *Science*, **285**, 397-400.

Lubow, B.C. & Ransom, J.I. 2016. Practical bias correction in aerial surveys of large mammals: validation of hybrid double-observer with sightability method against known abundance of feral horse (*Equus caballus*) populations. *PLoS ONE*, **11**, e0154902.

Machault, V., Vignolles, C., Pages, F., Gadiaga, L., Tourre, Y.M., Gaye, A., Sokhna, C., Trape, J-P., Lacaux, J-P. & Rogier, C. 2012. Risk mapping of *Anopheles gambiae s.l.* densities using remotely-sensed environmental and meterological data in an urban area: Dakar, Senegal, *PLoS ONE*, **7**, e50674.

Mulero-Pazmany, M., Barasona, J.A., Acevedo, P., Vicente, J. & Negro, J.J. 2015 Unmanned Aircraft Systems complement biologging in spatial ecology studies. *Ecology and Evolution*, **5**, 4808-4818.

Olsen, J.L., Miehe, S., Ceccato, P. & Fensholt, R. 2015. Does EO NDVI seasonal metrics capture variations in species composition and biomass due to grazing in semi-arid grassland savannas? *Biogeosciences*, **12**, 4407-4419.

Paneque-Gálvez, J., McCall, M.K., Napoletano, B.M., Wich, S.A. & Koh, L.P. 2014 Small drones for community-based forest monitoring: an assessment of their feasibility and potential in tropical areas. *Forests*, **5**, 1481–507.

Pettorelli, N., Laurance, W.F., O'Brien, T.G., Wegmann, M., Nagendra, H. & Turner, W. 2014. Satellite remote sensing for applied ecologists: opportunities and challenges. *Journal of Applied Ecology*, **51**, 839-848.

Pettorelli, N., Ryan, S., Mueller, T., Bunnefeld, N., Jedrzejewska, B., Lima, M. & Kausrud, K. 2011. The Normalized Difference Vegetation Index (NDVI): unforeseen successes in animal ecology. *Climate Research*, **46**, 15-27.

Pettorelli, N., Schulte to Buhne, H., Tulloch, A., Dubois, G., Macinnis-Ng, C., Queiros, A.M., Keith,D.A., Wegmann, M., Schrodt, F., Stellmes, M., Sonnenschein, R., Geller, G.N., Roy, S., Somers, B., Murray, N., Bland, L., Geijzendorffer, I., Kerr. J.T., Broszeit, S., Leitao, P.J., Duncan, C., El Serafy, G., He, K.S., Blanchard, J.L., Lucas, R., Mairota, P., Webb, T.J. & Nicholson, E. 2018. Satellite remote sensing of ecosystem functions: opportunities, challenges and way forward. *Remote Sensing in Ecology and Conservation*, **4**, 71-93.

Piggot, D.M. Golding, N., Mylne, A., Huang, Z., Henry, A.J., Weiss, D.J., Brady, O.J., Kraemer, M.U.G., Smith, D.L., Moyes, C.L., Bhatt, S., Gething, P.W., Horby, P.W., Bogoch, I.I., Brownstein, J.S., Mekaru, S.R., Tatem, A.J., Khan, K. & Hay, S.I. 2014. Mapping the zoonotic niche of Ebola virus disease in Africa. *eLife*, **10.7554**/eLife.04395.

Potvin, F. & Breton L. 2005. Testing two aerial survey techniques on deer in fenced enclosures – visual double counts and thermal infrared sensing. *Wildlife Society Bulletin*, **33**, 317–325.

Ramankutty, N., Evan, A.T., Monfreda, C. & Foley, J.A. 2008. Farming the planet: 1. Geographic distribution of global agricultural lands in the year 2000. *Global Biogeochemical Cycles*, **22**, GB1003.

Rizzoli, A., Neteler, M., Rosa, R., Wersini, W, Cristofolini, A., Brefoli, M., Buckley, A. & Gould, E.A. 2007. Early detection of tick-borne encephalitis virus spatial distribution and activity in the province of Trento, northern Italy. *Geospatial Health,* **2**, 169-176.

Sutton, P., Roberts, D., Elvidge, C. & Baugh, K. 2001. Census from Heaven: An estimate of the global human population using night-time satellite imagery. *International Journal of Remote Sensing*, **22**, 3061–3076.

Snapir, B., Waine, T.W. & Biermann, L. 2019. Maritime vessel classification to monitor fisheries with SAR: demonstration in the North Sea. *Remote Sensing*, **11**, 353.

Venter, O., Sanderson, E.W., Magrach, A., Allan, J.R., Beher, J., Jones, K.R., Possingham, H.P., Laurance, W.F., Wood, P., Feketa, B.M., Levy, M.A. & Watson, J.E.M. 2018a. *1993 Human Footprint, 2018 release*. Pallisades, NY: NASA Socioeconomic Data and Applications Center (SEDAC) https://doi.org/10.7927/H46H9938Z.

Venter, O., Sanderson, E.W., Magrach, A., Allan, J.R., Beher, J., Jones, K.R., Possingham, H.P., Laurance, W.F., Wood, P., Feketa, B.M., Levy, M.A. & Watson, J.E.M. 2018b. *2009 Human Footprint, 2018 release*. Pallisades, NY: NASA Socioeconomic Data and Applications Center (SEDAC) https://doi.org/10.7927/H46T0JQ4.

Walter, M.J. & Hone, J. 2003. A comparison of 3 aerial survey techniques to estimate wild horse abundance in the Australian Alps. *Wildlife Society Bulletin*, **31**, 1138-1149.

Wang, D., Shao, Q. & Yue, H. 2019. Surveying wild animals from satellites, manned aircraft and unmanned aerial systems (UASs): a review. *Remote Sensing*, **11**, 1308

Wang, Y., Huang, C., Feng, Y., Zhao, M. & Gu, J. 2020a. Using Earth observation for monitoring SDG 11.3.1- Ratio of land consumption rate to population rate in mainland China. *Remote Sensing*, **12**, 357.

Wang, D., Song, Q., Liao, W., Ye H., Shao Q., Fana, J., Cong, N., Xin, X., Yue H. & Zhang, H. 2020b. Integrating satellite and unmanned aircraft system (UAS) imagery to model livestock population dynamics in the Longbao Wetland National Nature Reserve, China. *Science of The Total Environment*, **746**, 140327.

Wang, J., Xiao, X., Bajgain, R., Starks, P., Steiner, J., Doughty, R. B. & Chang, Q. (2019) Estimating leaf area index and aboveground biomass of grazing pastures using Sentinel-1, Sentinel-2 and Landsat images. *ISPRS Journal of Photogrammetry and Remote Sensing*, **154**, 189-201.

Zhang, X., Saitoh, S.I. & Hirawake, T. 2017 Predicting potential fishing zones of Japanese common squid (*Todarodes pacificus*) using remotely sensed images in coastal waters of south-western Hokkaido, Japan. *International Journal of Remote Sensing*, **38**, 6129–6146.